SCIENTIFIC PAPER
Published: November 14, 2025
https://doi.org/10.13167/2025.31.12

Post-fire strengths and morphological properties of high-strength concrete reinforced with kenaf fibres

Oluwatobi Aluko[1,2]✉, Mariyana Abd Kadir[2,3], Paul Awoyera[4], Naraindas Bheel[5] and Jamaludin Yatim[2]

[1] *Ekiti State University, Faculty of Engineering, Iworoko, 362103, Ado Ekiti, Ekiti State, Nigeria*

[2] *Universiti Teknologi Malaysia, Faculty of Civil Engineering, 81310 Skudai, Johor, Malaysia*

[3] *Universiti Teknologi Malaysia, Institute of Noise and Vibration, 81310 Skudai, Johor, Malaysia*

[4] *Prince Mohammad Bin Fahd University, Faculty of Engineering, 31952, Al Kobar, Saudi Arabia*

[5] *AROR University of Art, Architecture, Design & Heritage Sukkur, 65170, Sindh, Pakistan*

Corresponding author:
Oluwatobi Aluko

Received:
January 2, 2025

Revised:
September 3, 2025

Accepted:
October 29, 2025

Published:
November 14, 2025

Citation:
Oluwatobi, A. et al. Post-fire strengths and morphological properties of high-strength concrete reinforced with kenaf fibres. *Advances in Civil and Architectural Engineering,* 2025, 16 (31), pp. 201-219. https://doi.org/10.13167/2025.31.12

ADVANCES IN CIVIL AND ARCHITECTURAL ENGINEERING (ISSN 2975-3848)

Faculty of Civil Engineering and Architecture Osijek
Josip Juraj Strossmayer University of Osijek
Vladimira Preloga 3
31000 Osijek
CROATIA

Abstract:
The high manufacturing cost of conventional fibres and the need for greener and more sustainable constructions necessitate the adoption of plant-based fibres in concrete. Previous research has shown that fibres remarkably influence the post-fire behaviour of concrete. Post-fire concrete strengths and micro-imageries are vital to the serviceability requirements of concrete. Therefore, this paper presents an experimental report on a 28-day cured kenaf fibrous high-strength concrete (KFHSC), heated from ambient temperature to 800 ºC at 100 ºC intervals, sustained for 1, 2, and 3 h, and tested after being cooled naturally to ambient temperature. The fibres were treated and examined through SEM to ascertain their interfacial properties. Test samples of concrete grade 60 were prepared using an optimum volume (0,75 %) and length (25 mm). The KFHSC's residual strength characteristics, weight, ultrasonic pulse velocity, and morphology were determined and compared with plain (unreinforced) high-strength concrete. The findings show that samples of both mixes degraded with an increase in temperature and exposure durations. However, kenaf fibre retrained crack extension at a lower temperature phase and through networks of channels within the matrices, reduced pore pressure build-up at a higher temperature phase and consequently lessened the explosive spalling of the heated concrete.

Keywords:
biofibres; kenaf fibre; residual mechanical properties; microstructures; elevated temperature

1 Introduction

High-strength concrete (HSC) is becoming increasingly popular because of its high resistance to compressive stresses with minimal thickness demands for specific segments, which lowers the weight of the structure. Manufacturing it requires a high proportion of cement with a low water–cement ratio and water-lessening admixtures [1]. Additionally, fibre contributes significantly to the creation of tougher and more durable concrete that deteriorates less owing to cracks, corrosion, and fire impact; however, the high cost of manufacturing commonly used fibres and the need for greener composites engendered the use of biofibres in concrete. For more than four decades, plant-based fibres derived from cotton, hemp, jute, bamboo, flax, ramie, coconut, sisal, bagasse, and kenaf have been incorporated into concrete with notable enhancements in characteristics and more research possibilities [2-4].

Fibres, particularly hybrids of metallic and polypropylene fibres, have been shown to improve the fire behaviour of HSC by reducing the buildup of vapour pressure and crack propagation [5-7]. However, previous studies have shown that biofibres in concrete reduce crack propagation and pore-pressure buildup in heated concrete, in addition to providing sustainability, CO2 neutrality, and relatively high stiffness [3; 8; 9]. However, the behaviour of biofibrous concrete exposed to high temperatures has not been studied extensively. Nonetheless, only a few studies focused on normal-strength concrete using hemp fibres [10] heated up to 400 °C. Studies found that hemp fibres had no discernible effect on the retained characteristics of the concrete, and hemp fibres that were only partially broken may have slowed the spread of cracks. In addition, HPC and ultra-high-performance concrete (UHPC) incorporating jute have been studied, and the studies found that in contrast to 3 kg/m^3 for polypropylene fibres, 10 kg/m^3 of jute fibres is required to lessen the UHPC spalling tendency [11; 12]. Thus, jute fibres can be used as a spalling-mitigation measure in high-performance concrete.

Moreover, the synergistic advantages of biofibres and steel fibres were explored. A study [13] examined the impacts of bamboo fibres on UHPC at high temperatures, focusing on the blend of bamboo and steel fibres, with different fibre compositions (0-2 % steel fibres, 0-1,5 % bamboo fibres), the UHPC samples were exposed to temperatures of 200, 400, 600, and 800 °C. According to the results, the bamboo fibres considerably improved the crack resistance and anti-spalling characteristics. Bamboo fibre carbonisation produced channels that reduced steam pressure and thermal stress between 400 and 600 °C, preventing cracks from spreading and spalling. The hybrid fibre system demonstrated lower porosity, less fracture growth, and preserved compressive strength compared with steel fibre-only UHPC. By reducing the internal stresses caused by uneven thermal expansion, bamboo fibres help increase the overall thermal endurance of the material. A similar study [14] examined the combined effects of steel fibres (SF) and bamboo fibres (BF) on the mechanical and spalling properties of UHPC subjected to high temperatures using 25 mixes of five different contents of BF (0,0; 2,5; 5,0; 7,5; and 10,0 kg/m^3) and five of SF (0, 1, 2, 3, and 4 %), exposed to temperature that ranged from 25 to 800 °C. The results showed that a low hybrid content of BF and SF completely prevented UHPC from spalling; using either SF or BF alone was unable to stop spalling at high fibre levels. Furthermore, the increase in the permeability of BFs and the bridging function of SF caused a synergistic beneficial effect of BF and SF on the spalling resistance of UHPC. No reports have been published on HSC reinforced with biofibres, which are also prone to explosive spalling owing to their dense microstructure. Hence, such a study is required.

Originating in Africa, the kenaf plant, an ancient (4000 years old) herbaceous plant and part of Hibiscus Cannabinus (family Malvaceae), similar to the cotton plant [8], is the source of kenaf fibre. It is widely and commercially grown in Malaysia, where this study was conducted, and its high yield, tensile strength, low density, high aspect ratio, and modulus make it useful [8]. Recent studies have found that kenaf fibres are beneficial, and research on fibre characterisation, composite creation, and usage in construction has been conducted on kenaf fibre-reinforced concrete [3; 15;16]. It saves energy because 1 kg of glass fibre requires 54 MJ of energy to make compared with 15 MJ for kenaf [3]. Biofibrous concrete exhibits better

functionality at room temperature, and its efficacy at higher temperatures is currently a primary area of investigation.

The durability and capability of kenaf fibres in HSC under thermal stress must also be considered in the search for biofibrous building materials. The serviceability requirements of fire-damaged HSC are significantly influenced by the strength and microstructure. Other biofibres such as hemp, jute, and Spanish-broom fibres in composites have been studied [10-12; 17]. Additionally, the retained strength characteristics and matrix structures of kenaf fibrous high-strength concrete (KFHSC) should be studied at the micro level. Therefore, this study investigated KFHSC of grade 60, exposed to thermal loads up to 800 ºC, maintained for 1, 2, and 3 h, and tested after cooling using the unstressed residual testing technique. The ultrasonic pulse velocity (UPV), weight loss, morphology, and residual mechanical characteristics of the KFHSC were measured and compared with those of plain high-strength concrete (PHSC). In addition to using the data obtained in this study in the biocomposite construction sector, it can also be used to build standards for design and application strategies.

2 Methodology

2.1 Materials

The materials used for this research included aggregates, cement, kenaf fibre, potable water, and a superplasticiser. Kenaf was obtained from the National Tobacco Board in Kelantan, Malaysia. However, because of the hygroscopic and hydrophilic nature of kenaf fibres, modification of the fibres through alkaline treatment was necessary before they could be used in a concrete mixture. The fibres were treated with an optimum alkaline concentration of 5 % NaOH. At ambient temperature, the fibre samples were kept in the alkaline solution for 3 h for adequate mercerization, after which the fibres were washed and kept in fresh water for 24 h to completely remove the alkaline solution. This treatment removes impurities such as waxes, oil, and pectins, consequently improving the surface roughness of the fibre-concrete matrix affinity [18]. The fibres were air-dried, combed, and chopped to 25 mm, as shown in Figure 1a), before adding 0,75 % volume to the mixture.

Figure 1a) shows the treated, short discrete kenaf fibre, and Figure 1b) shows that the alkaline solution removed the wax and oil protecting the outer face of the fibre cell wall and the hydrogen bonding in the interconnected structure of fibre cellulose, hemicellulose, and lignin, thereby improving the fibre surface roughness and interfacial properties. The interfacial properties of a fibre are crucial for its function in a cementitious matrix. Figure 1c) shows the untreated kenaf fibres. The smooth surface of the untreated fibre is shown in Figure 1d), which shows the network of cellulose, wax, and oil covering the surface, as reported in a previous study [10] on hemp fibre modification.

Figure 1. Kenaf fibre: a) treated, b) SEM (treated), c) untreated, and d) SEM (untreated)

The physical and strength characteristics of the kenaf fibres used in this study were obtained through tests [19]; the test results are presented in Table 1. River sand with a maximum grain size of 4,75 mm was used as the fine aggregate, and crushed granite of 10 mm was used; both fine and coarse aggregates were well graded, following the standard [20]. Ordinary

Portland cement (OPC, 142.5) and RHEOBUILD 1100 superplasticiser were used according to existing standards [21].

Table 1. Characteristics of alkaline-treated kenaf fibres [22]

Fibre characteristics	The values
diameter (μm)	40-115
length (mm)	25
average aspect ratio	500 μm
tensile strength (MPa)	136-930
elastic modulus (GPa)	15-54
elongation at yield (%)	1,60-1,77
density (kg/m^3)	1,05-1,52

2.2 Concrete mixing and sample preparation

For this investigation, two mixes of 264 samples were prepared for UPV, compressive strength, and split tensile tests at ambient and elevated temperatures using the Department of the Environment's (DOE) mix design approach. Twelve cubical and cylindrical concrete samples were prepared for the ambient assessment of the control and kenaf fibre concrete mixtures, whereas 252 samples comprising cubes and cylinders were prepared for heat treatment. The mix designs are presented in Table 2. The mixing process used to prepare the KFHSC specimens was slightly different from the ordinary concrete mixing procedure because of the addition of kenaf fibres. Before the mixing process, short, distinct kenaf fibres were soaked for 30 min [23]. This was performed to hydrate the fibres to avoid affecting the already designed water–cement ratio of the mixture. All the aggregates were poured into a mixing drum and mixed before the addition of cement and water. Subsequently, the fibres were gradually added in small amounts and the mixture was blended for five minutes. A dosage of superplasticiser was added and mixed for five minutes to ensure consistency of the mixture and to mitigate the 'balling' effect in the KFHSC mixture, which is one of the commonest problems with cementitious biocomposites [24]. After casting, a vibrating table was used to properly compact the fresh specimens, which were then demoulded after 24 h, as shown in Figure 2, and cured in water for 28 days. The samples were then dried at room temperature, weighed, and tested.

Figure 2. Demoded cube and cylindrical samples

Table 2. Concrete mix design

Mixes	PHSC	KFHSC
kenaf fibre (%)	0	0,75
kenaf fiber (kg/m^3)	0	9
water (w/c=0,33) (kg/m^3)	250	250
cement (kg/m^3)	532	532
fine agg. (kg/m^3)	688	688
coarse agg. (kg/m^3)	875	875
SP (1 %)	5,32	5,32

2.3 Concrete furnace treatment

One method to determine the aversion of concrete to fire is through standard fire tests [25; 26]. However, this study used an unstressed residual testing procedure, which lets samples to cool to ambient temperature before being loaded to failure to obtain the strength properties; this procedure is comparable to those in previous studies [19; 20]. Each category of KFHSC samples (cubes, and cylinders) along with the control samples were heated to 100, 200, 300, 400, 600, and 800 °C and for 1, 2 and 3 h of heating cycles in a furnace (muffle cardiolite) that was powered electrically. as shown in Figure 3. The heating rate was 4,1 °C/min for 1, 2, 3 h, as shown in Figure 4, like some previous studies [27,28]. The samples were allowed to cool naturally to room temperature, and the cooling was monitored with a portable Reed Infrared thermometer; the average cooling rate was 49 °C/min for the 800 ºC samples. The weight loss, UPV, compressive strength, and splitting tensile strength of the samples were examined.

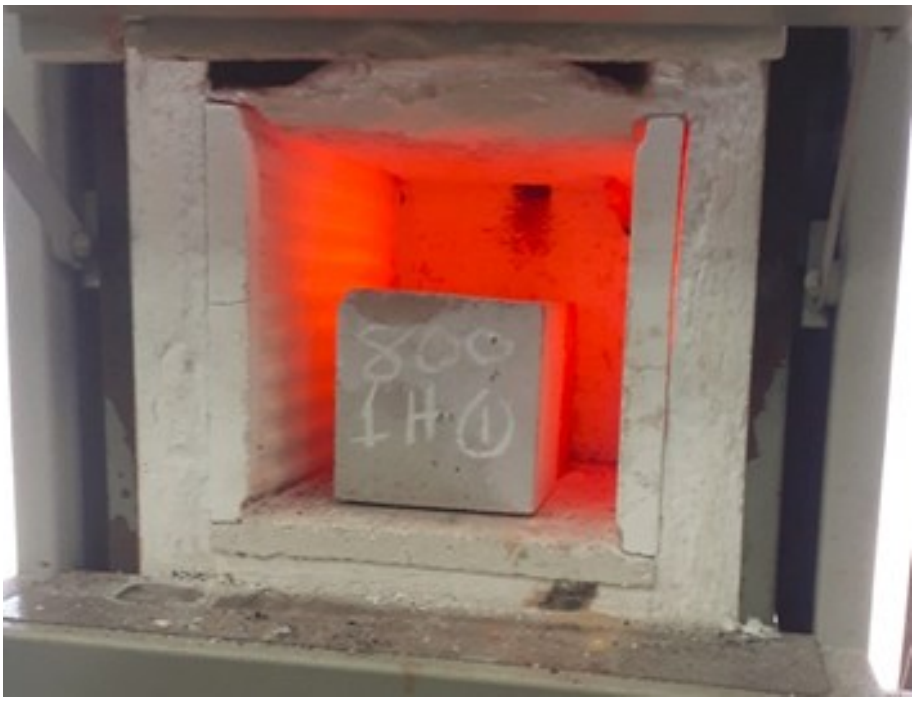

Figure 3. Cube sample in a furnace

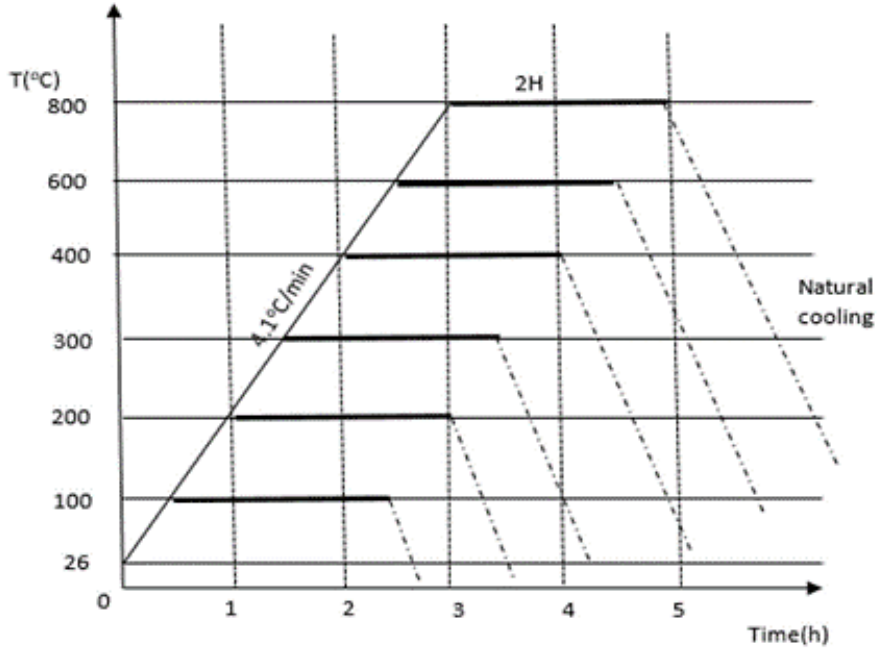

Figure 4. Temperature–time heating curve for the samples

2.4 Tests on hardened heated samples

Each test was conducted in Malaysia at the Universiti Teknologi Malaysia's D04 Faculty of Civil Engineering. The samples were subjected to UPV to compare the pre- and post-furnace heating integrity of the KFHSC and PHSC. The weight loss in the KFHSC cube samples was ascertained by calculating the pre- and post-furnace heating weight differences, expressed in percentages as a function of the increased temperatures for the 1, 2, and 3 h exposures. A compressive strength test based on [29] was conducted using a 2500 kN compression machine with a loading rate of 6 kN/s. Air-cooled 100 mm cube KFRC samples were tested under the compression machine, as shown in Figure 5a), for each targeted temperatures (100, 200, 300, 400, 600, and 800 °C), and the average values were recorded as the residual strengths. The average UPV test results for each target temperature were also estimated as a function of the elevated temperature and exposure period.

a) b)

Figure 5. a) Compressive strength loading, b) splitting tensile loading

The same machine used for the compressive strength test was used for the split tensile strength test based on a previous study [30]. Cylindrical samples (100 diameters and 200 mm

height) were loaded at a rate of 1,25 kN/s using the same machine, but the jaw was changed, and the samples were packed with a plywood plate at the lower and upper parts of the jaw. The average and relative residual strengths were obtained for the compressive and split tensile strengths, where the relative residual strength at a given temperature was the residual strength ratio at different target temperatures to the strength at ambient temperatures. The microstructures of the samples were examined using scanning electron microscopy (SEM, JEOL JSM-IT300LV) at a working voltage of 20 kV.

3 Results and discussion

Because different material compositions and temperature variations affect the performance of concrete differently, strength characteristics continue to be the most important characteristics of concrete subjected to high temperatures [31]. The test results presented in this section include the weight loss, residual UPV, compressive strength, and split tensile strength, which demonstrate the decrease in concrete strength with temperature variation and exposure times.

3.1 Result of residual UPV

Because of its lower density than that of PHSC, kenaf fibre had a noticeable effect on the UPV results of KFHSC. Figure 6 shows the UPV values for KFHSC and PHSC at room temperature, which were 4,786 and 4,856 km/s, respectively. A higher value of 1,5 % for PHSC indicates good concrete quality [32]. Both combinations underwent a slow transformation before 400 ºC. Nevertheless, at 400 ºC and above, the UPV values for KFHSC and PHSC decreased dramatically. Hence, KFHSC and PHSC lost 22 %, 19 %, 7 2%, and 68 % of their pre-heating values at 800 and 400 ºC for 1 h exposure, respectively. As shown in Figure 6, the effects of the exposure temperature and time became significant for 2 h exposure.
Consequently, the KFHSC and PHSC lost 28 % and 24 % of their pre-heating values at 400 ºC and 78 % and 71 % of their UPV values at 800 ºC, respectively. Over three hours, both samples degraded at 800 ºC, losing 82 % (0,842 km/s) and 76 % (1,187 km/s) of their original values, respectively. Both mixes were considered to experience microstructure coarsening due to fire impact [27]; therefore, the decline in the KFHSC UPV was not solely attributable to the ashing of kenaf fibres, but rather to the breakdown of C-S-H at 450 ºC, which made the matrices more porous and permeable, lowering the sample's UPV values. Figure 7 shows the UPV values based on the temperature relative to the ambient temperature. Table 3 also shows the proposed models for two of the six curves, with R^2 = 0,996 and 0,992, respectively.

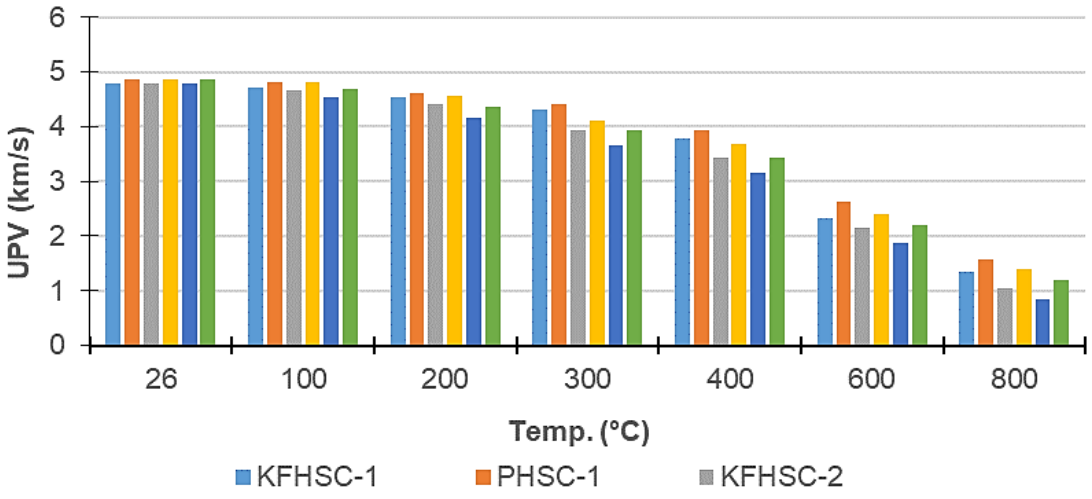

Figure 6. Residual UPV vs. temperature changes and exposure period

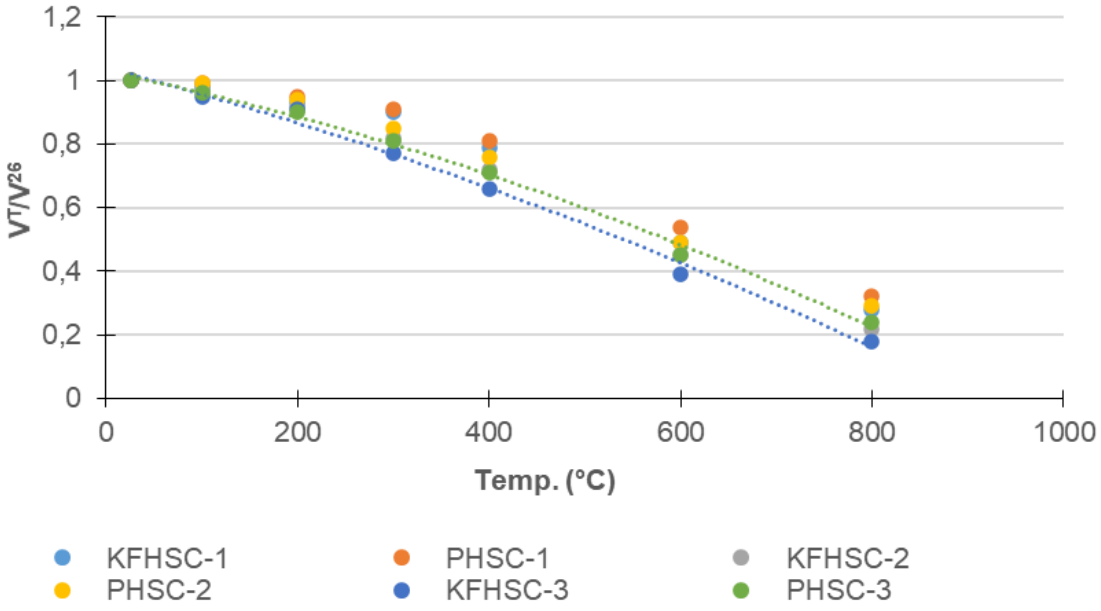

Figure 7. Relative residual UPV vs. temperature for 1, 2, and 3 h

Table 3. Proposed models for relative residual UPV

Mixture	Model	R^2
KFHSC-3	$\frac{V^T}{V^{26}} = -4 \times 10^{-7}T^2 - 0{,}0008T + 1{,}0397$	0,992
PHSC-3	$\frac{V^T}{V^{26}} = -5 \times 10^{-7}T^2 - 0{,}0006T + 1{,}028$	0,996

3.2 Weight loss

Concrete degradation can be estimated by calculating the weight loss [33]. Figure 8 illustrates the effects of the exposure temperatures and duration on the weight of the KFHSC and PHSC samples. At room temperature, the KFHSC samples were lighter than the PHSC samples because kenaf fibres have a lower specific gravity than steel fibres. After an hour of heating between 26 and 300 °C, both mixes slightly lost their weight, which may have been caused by the samples becoming dehydrated, as confirmed in a similar study [34].
KFHSC and PHSC lost 2,5 % and 2,1 % at 300 °C and 9,4 % and 8,4 % at 800 °C, respectively. For a two-hour exposure period, both mixes lost weight between 26 and 300 °C, but KFHSC's loss was particularly noticeable. At 300 °C, KFHSC and PHSC lost 4,6% and 3,1 %, respectively. KFHSC lost weight significantly at 800 °C (9,6%) as opposed to PHSC (8,8 %). Moreover, Figure 7 illustrates that weight loss was more significant for 3 h heating compared with that for 1 and 2 h. At 300 ºC, KFHSC lost 4,7 %, whereas PHSC lost 3,5 %. At 800 ºC, KFHSC lost 9,9 %, whereas PHSC lost 8,8 %. At this temperature, the kenaf fibres in the KFHSC samples were completely broken down, and the cement paste and aggregates dried in both mixes. In addition to fibre deterioration, the lower density and higher permeability matrix of KFHSC dehydrates more quickly than samples with higher densities, which is the cause of greater weight loss. This discovery is consistent with the use of hemp fibre [10], the disintegration of concrete components at high temperatures, the release of bound water from the cement paste, and the porosity of concrete [35].

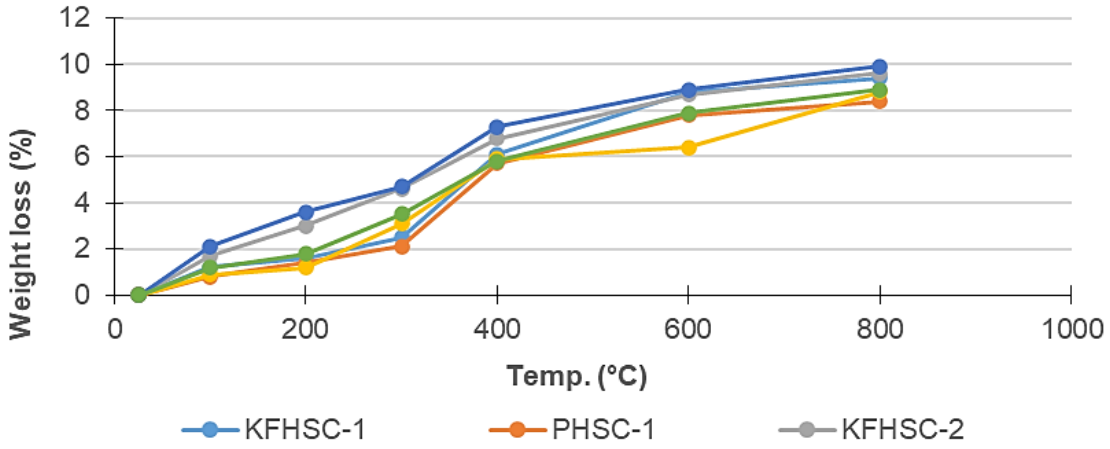

Figure 8. Average weight losses vs. temperature changes and exposure periods

3.3 Residual compressive strength test

Figure 9 shows the relative compressive strengths of the KFHSC and PHSC mixes for various temperatures and exposure durations. Note that kenaf fibre did not increase the compressive strength of the KFHSC mix, even at room temperature, which is typical for all biofibres. This could be explained by the balling effect in fresh concrete, low specific gravity, and the inability to distribute the fibre evenly in the mix. Consequently, the strength enhancement experienced on the composite was a regular concrete strength spike initiated at a particular temperature level owing to the hydration of the remaining unhydrated cement within the composite [36].
The strengths of KFHSC and PHSC increased by 1 % and 2 % at 100 °C, respectively, after 1 h exposure, as shown in Figure 8, which was consistent with a similar report [37]. A possible explanation for the slight increase in compressive strength is that the samples were dehydrated in a lower temperature range, which created van Der Waals forces before boosting the strength. Moreover, calcium hydro-silicate (C-S-H) and $Ca(OH)_2$ are exuded, and the release of chemically bound free water is accelerated. Nevertheless, a 14% and 13% decrease was observed in the KFHSC and PHSC strength at 200 °C respectively. A possible explanation for this is that the water content of the samples decreased, creating voids that reduced their compressive strengths. This phenomenon is known as a 'strength recession' [38]. The KFHSC and PHSC strengths increased by 6 % at 300 ºC compared with that at 200 ºC. This could be because the hydration phase was exhausted, enabling vaporised water to move through the pores and voids of the unhydrated cement, forming greater bonds within the KFHSC matrix. PHSC and KFHSC recovered to 99 % and 97 % at 400 ºC, respectively, and both KFHSC and PHSC lost 48 % and 37 % of their initial strength at 600 ºC and 76 % and 68 % at 800 ºC, respectively.
Comparably, both mixtures increased in strength by 2 % at 100 ºC and decreased by 12 % and 11 % at 300 ºC, respectively, after 2 h of exposure, as illustrated in Figure 9. At 400 ºC, the compressive strength decreased by only 8 % and 7 % for KFHSC and PHSC, respectively. At 800 ºC, KFHSC and PHSC lost 71 % and 80 % of their room-temperature strength, respectively. Figure 8 depicts the results for a 3 h duration. At 100 ºC, both mixtures gained 2 % strength, but their strengths declined quickly. At 800 ºC, KFHSC and PHSC lost 83% and 76 % of their room-temperature strength, respectively. The creation of further hydration products through the change from the C-S-H state to the pectolite state [$NaCa_2Si_3O_8(OH)$]. The first stage of aggregate and C-S-H disintegration began at 600 oC, and the second stage of C-S-H disintegration and β-C2S generation occurred between 400 and 800 ºC for both mixes. To the best of our knowledge, no reports have been published on the effects of elevated temperatures and exposure periods on biofibrous concrete to validate this finding. However, previous reports [10; 12; 17] have revealed comparable outcomes for 1, 2, and 3 h exposures

for hemp, jute, and Spanish broom fibres, respectively. Thus, we can conclude that the KFHSC strength reduction is a result of concrete material degradation rather than a fibre effect [12].

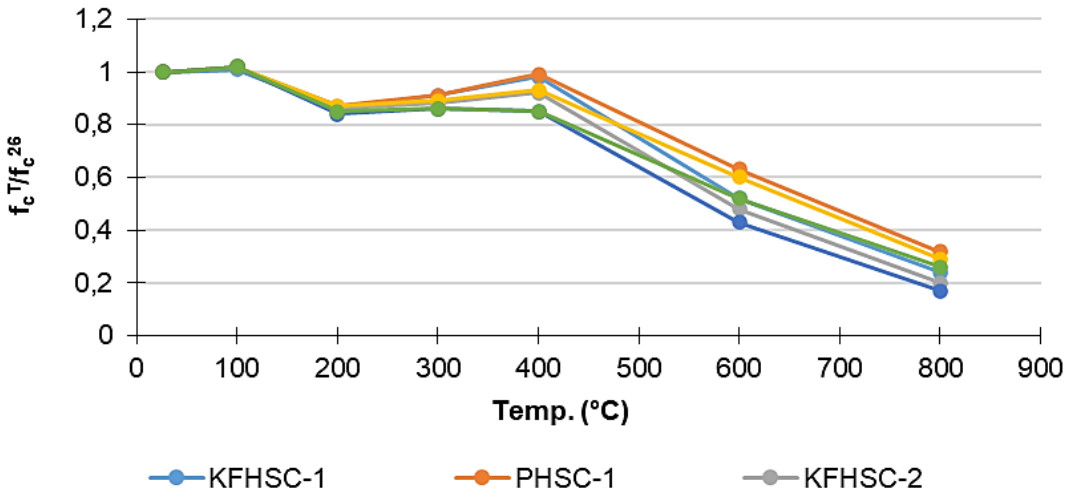

Figure 9. Relative residual compressive strength vs. temperature changes and exposure period

Figure 10 shows the relationship between the compressive data for KFNSC and KFHSC, with their control samples between 26 to 800 ºC for 3 h. The curves in the graphs were tested for fit, and the highest one with R2 was selected. Polynomial regression curves were obtained for $(f_c^T)/(f_c^{26})$, as shown in Figure 10, which indicates that $(f_c^T)/(f_c^{26})$ decreased with increasing temperature. Increases in temperature and exposure duration significantly influenced the relative residual compressive strength. The proposed equations for the compressive strength are presented in Table 4.

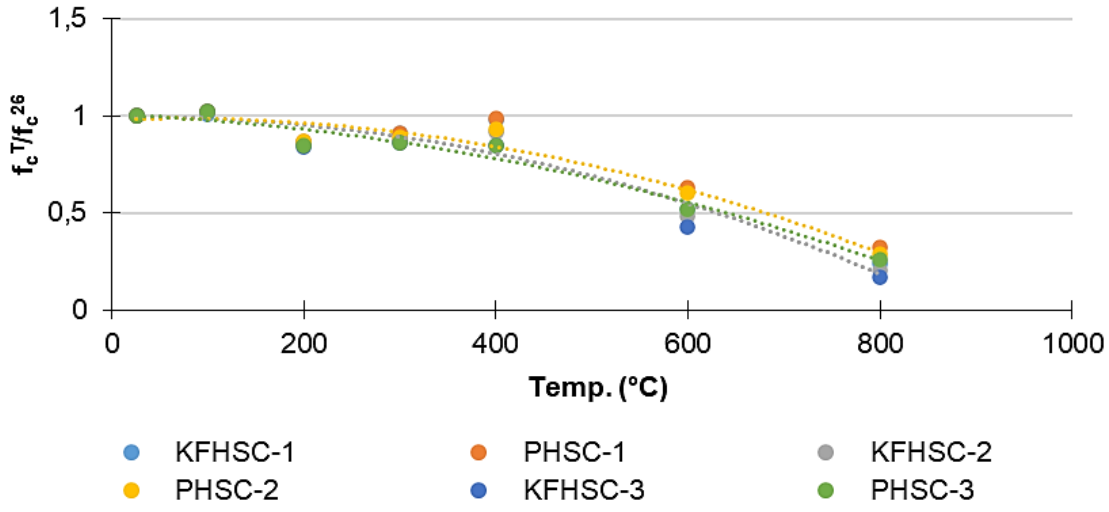

Figure 10. Relative residual KFHSC compressive strength vs. temperature change for 1, 2, and 3 h

Table 4. Models for relative residual compressive strength

Mixture	Model	R^2
KFHSC-2	$\frac{f_c^T}{f_c^{26}} = -1 \times 10^{-6}T^2 + 7 \times 10^{-5}T + 0{,}9927$	0,950
PHSC-2	$\frac{f_c^T}{f_c^{26}} = -10^{-6}T^2 + 0{,}0002T + 0{,}9821$	0,955
KFHSC-3	$\frac{f_c^T}{f_c^{26}} = -1^{-6}T^2 - 0{,}0002T + 0{,}9821$	0,962
PHSC-3	$\frac{f_c^T}{f_c^{26}} = -9 \times 10^{-7}T^2 - 0{,}0002T + 1{,}007$	0,968

3.4 Residual splitting tensile strength test

Concrete containing kenaf fibres has a significant benefit in terms of tensile stress resistance. The cylindrical KFHSC samples displayed only minor surface cracks and withstood abrupt failure or complete breakage. The KFHSC and PHSC exhibited a 4% strength enhancement at 100 ºC, as illustrated in Figure 11; however, as the temperature and duration increased, the split tensile strength decreased rapidly. The room-temperature values of KFHSC and PHSC decreased by 23 % and 17 % at 400 ºC and 72 % and 66 % at 800 ºC, respectively. Over two hours of exposure, only a slight increase in their strength by 2 % at 100 ºC and 100 % strength recovery at 100 ºC after 3 h was observed. However, both mixes lost 81 % and 76 % of their initial strength at 800 ºC. Figure 11 illustrates the loss in the pre-heating strength of both mixes of 87 % and 81 % at 800 ºC for a 3 h exposure period. The behaviour of KFHSC between 26 and 400 °C was consistent with the earlier discovery [28] that used Alfa fibre, in contrast to non-fibrous samples. When concrete is exposed to indirect tensile stress, kenaf fibres absorb the tensile force and stop progressive cracking through stress distribution and bridging mechanisms. The capacity of kenaf fibres to span fissures in the concrete matrix offers some post-cracking ductility and prevents cracks from spreading further. Consequently, this caused the improvement in tensile splitting strength of KFHSC at the lower temperature phase (100-300 °C).

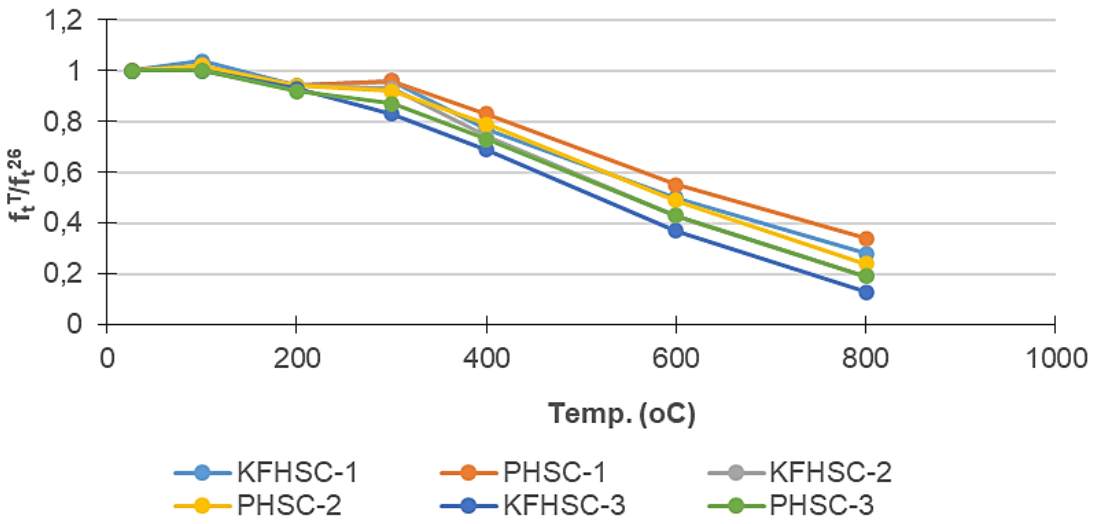

Figure 11. Relative residual splitting tensile Strength vs. temperature changes and exposure period

Figure 12 shows the correlation between the relative residuals of the split tensile strength (KFHSC and PHSC) data and the temperature variations for 1 and 3 h. The highest one with

R2 was selected after the fitting. Linear and polynomial regression curves were obtained for $(f_t^T)/(f_t^{26})$, as shown in Figure 12, which indicates that $(f_t^T)/(f_t^{26})$ decreased with increasing temperature. The relative residual tensile strength was significantly influenced by an increase in temperature and exposure duration. The proposed equations for tensile strength are listed in Table 5.

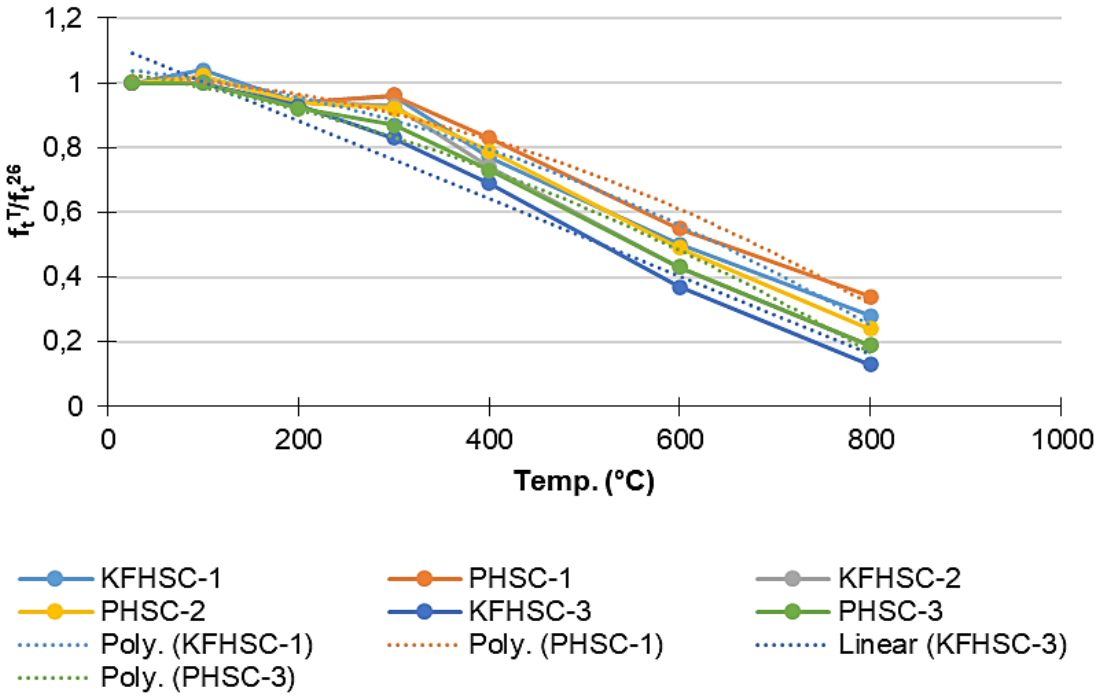

Figure 12. Relative residual splitting tensile strength with temperature for 1, 2, and 3 h exposures

Table 5. Proposed model for relative residual split tensile strength

Mixture	Model	R^2
KFHSC-1	$\frac{f_t^T}{f_t^{26}} = -0{,}0012T + 1{,}1235$	0,971
PHSC-1	$\frac{f_t^T}{f_t^{26}} = -10^{-6}T^2 - 0{,}0001T + 1{,}0236$	0,981
KFHSC-3	$\frac{f_t^T}{f_t^{26}} = -9 \times 10^{-7}T^2 - 0{,}0003T + 1{,}0444$	0,974
PHSC-3	$\frac{f_t^T}{f_t^{26}} = -8 \times 10^{-7}T^2 - 0{,}0004T + 1{,}0374$	0,991

3.5 Relative residual compressive and split tensile strength of KFHSC and PHSC

To clarify the strength degradation, Table 6 summarises the residual strength for the compressive split tensile strength.

Table 6. Relative residual strength of the KFHSC and PHSC with temperature changes

	Mixture	Heating duration (hrs)	Temperature (°C)						
			26	100	200	300	400	600	800
compressive strength (kN/mm^2)	KFHSC	1	1,00	1,01	0,86	0,91	0,98	0,52	0,24
		2	1,00	1,02	0,86	0,88	0,92	0,48	0,20
		3	1,00	1,02	0,84	0,86	0,85	0,43	0,17
	PHSC	1	1,00	1,02	0,87	0,91	0,99	0,63	0,32
		2	1,00	1,02	0,87	0,89	0,93	0,60	0,29
		3	1,00	1,02	0,85	0,86	0,85	0,52	0,26
split tensile strength (kN/mm^2)	KFHSC	1	1,00	1,04	0,94	0,96	0,77	0,50	0,28
		2	1,00	1,02	0,94	0,93	0,74	0,43	0,19
		3	1,00	1,00	0,93	0,83	0,69	0,37	0,13
	PHSC	1	1,00	1,02	0,94	0,96	0,83	0,55	0,34
		2	1,00	1,02	0,94	0,92	0,79	0,49	0,24
		3	1,00	1,00	0,92	0,87	0,73	0,43	0,19

3.6 Microstructure

Figure 13a) and b) show the KFHSC and PHSC before heating. Both mixes were reasonably dense, stable, and unaltered at ambient temperature, except for some cracks around the kenaf fibres in the KFHSC matrix owing to fibre pull-out, as shown in Figure 13a). For the PHSC, as presented in Figure 13b), C-S-H was well formed on the matrices. With increasing temperature and exposure duration, the microstructure of the KFHSC matrix underwent a notable transformation. Hence, this section discusses the morphological properties of KFHSC compared with PHSC for 1, 2, and 3 h exposure at ambient and critical temperatures (400 and 800 ºC).

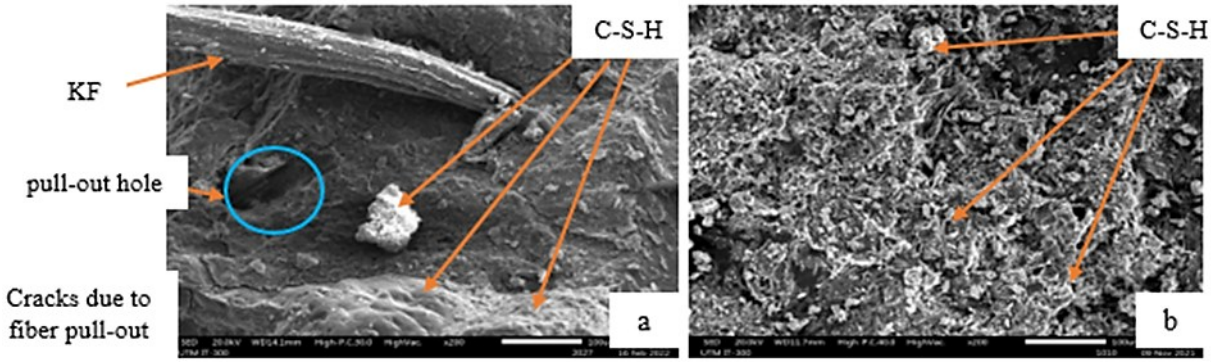

Figure 13. Micrograph (100 µm) at room temperature: a) KFHSC, b) PHSC

3.6.1 Microstructures at 400 ºC for 1, 2, and 3 h exposure

The microstructure of KFHSC after 1, 2, and 3 h of exposure at 400 ºC is shown in Figure 14 (a–f). The role of kenaf fibres in matrix cracks and spalling-reduction capability compared with PHSC is also shown. For the 1 and 2 h exposures, as shown in Figures 14a) and b) and c) and d), no cracks were observed on either matrix at this exposure temperature and duration. In the KFHSC matrix, some kenaf fibres were observed, which were considered to provide a bridging mechanism and crack mitigation. However, no significant cracks were found in the PHSC matrix, except for a few microvoids. This agreed with a previous microstructural study [10] on a hemp fibre cementitious composite for 1 h exposure. As shown in Figure 14a) and c), although some voids were observed beneath the kenaf fibres, they were not thermally induced, but rather resulted from the bridging action of the kenaf fibres during the mixing of the

concrete, which also reduced the density of the matrix. Kenaf fibres most likely possessed thermal endurance because of the alkaline treatment. This improved the thermal performance according to a previous study [11]. C-S-H crystallised in both mixes, which led to an increase in the compressive strength measured at this temperature.

Additionally, the strength increased more by the conversion of the C-S-H gel to crystalline phases than by the initial C-S-H gel. Consequently, a denser microstructure was produced by a new crystalline segment containing free lime formed during cement hydration. This must have been attributed to the increases in the KFHSC and PHSC compressive strengths of 13 % and 14 % at 400 ºC, respectively, owing to the increased solid volume and bond strength. As illustrated in Figure 14e) and f), for 3 h, the kenaf fibre deteriorated, although a few small ones might stop cracks from spreading. Nevertheless, some microcracks were observed in both the KFHSC and PHSC samples, and the cement paste of the matrix had a long crack line, as shown in Figures 14e and f). The autoclaving process in the cement paste became ineffective, probably due to the duration, which also affected the strength because the surge in compressive strength was only for 1 and 2 h, excluding the 3 h exposure. A long exposure duration was observed with no crystallised C-S-H in either matrix; 3 h exposure affected the matrices, and the enhancement in the compressive strength of both matrices was marginal.

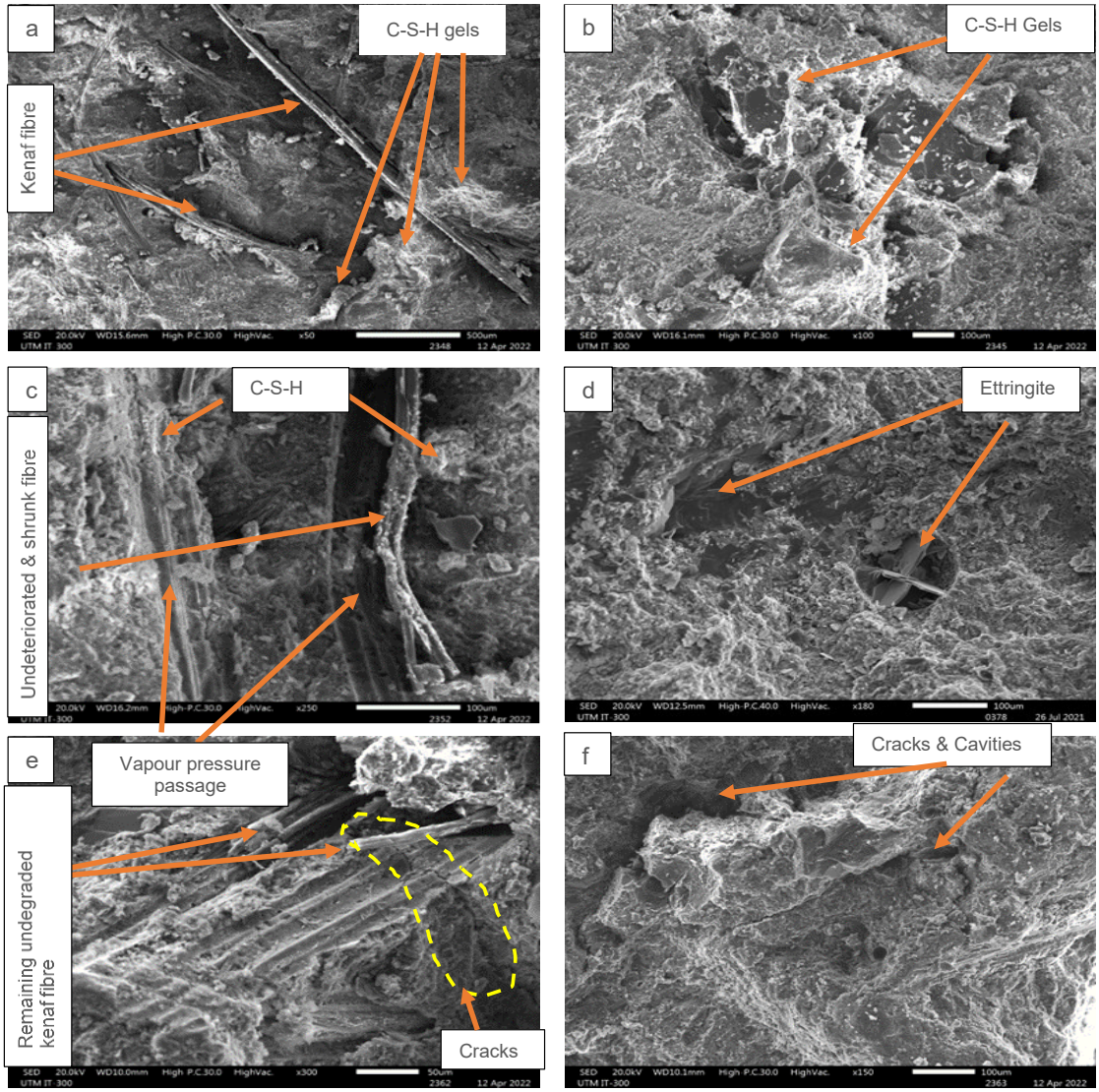

Figure 14. Micrograph (100 µm) at 400 ºC: a) KFHSC-1H, b) PHSC-1H, c) KFHSC-2H, d) PHSC-2H, e) KFHSC-3H, and f) PHSC-3H

3.6.2 Microstructures at 800 ºC for 1, 2, and 3 h exposure

A 'bridging' function was observed from partially deteriorated, shrunk KF at 800 ºC for 1 h exposure, as illustrated in Figure 15a). However, here, β-C2S was the result of the second stage of CSH breakdown. When the cement paste and aggregates were completely dehydrated, the microstructure became more porous and laden with microcracks, leading to cement paste shrinkage and aggregate expansion. However, PHSC exhibited more microcracks than KFHSC, as shown in Figure 15 (b). This is similar the particle boards suggested by Hager [36] as a method to reduce thermal spalling in hot concrete. As observed in Figure 15a), the partially deteriorated kenaf fibre might have served as an 'expansion joint.' Because of their low thermal conductivity, the heated samples experienced less thermal stress. In contrast, the PHSC exhibited persistent aggregate expansion and cement paste shrinkage, which led to significant cracks in the sample, as shown in Figure 15b). Additionally, the kenaf fibre's contraction at this temperature permitted the passage and release of vapour pressure, which in turn reduced the likelihood of spalling caused by the formation of pore pressure. A comparable study on jute fibres was reported [12], although the spalling of PHSC was less pronounced at this temperature and exposure.

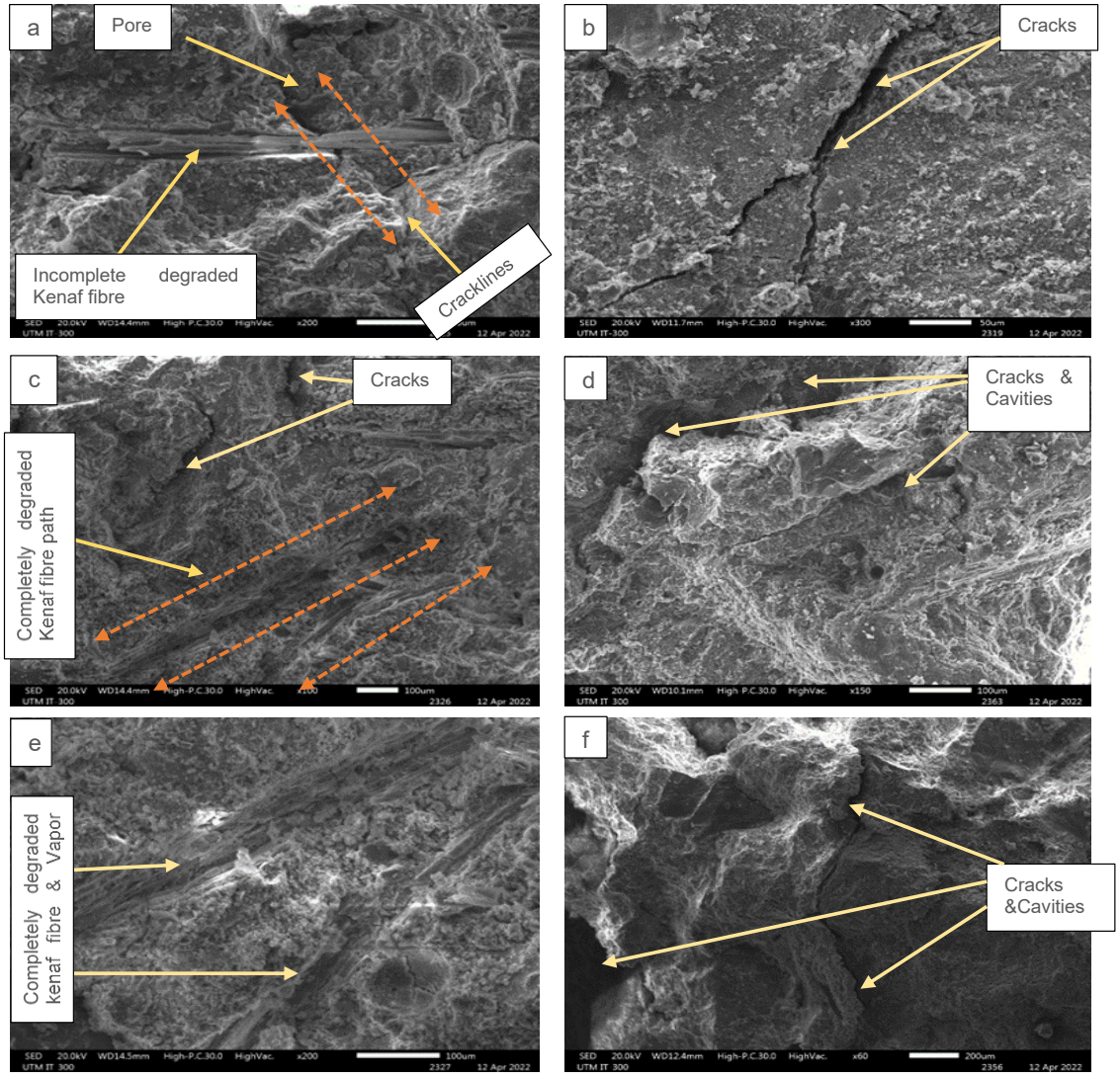

Figure 15. Micrograph (100 µm) at 800 ºC: a) KFHSC-1H, b) PHSC-1H, c) KFHSC-2H, d) PHSC-2H, e) KFHSC-3H, and f) PHSC-3H

According to Figures 15c) and d), kenaf fibres were fully broken down and produced gaps and cracks in the matrix after being exposed for 2 h for both the KFHSC and PHSC. The observed crack propagation can be partly attributed to the full dehydration of the matrix. Cavities and fissures were observed throughout the PHSC matrix. At this stage, full C-S-H decomposition was feasible for KFHSC and PHSC. Figures 15c) and d) show the change of the matrix into an amorphous structure, causing more fractures and voids to emerge throughout the concrete samples. C-S-H deteriorated. According to Figures 15e) and f), kenaf fibres were fully broken down and produced gaps and cracks in the matrix after being exposed for 2 h for the KFHSC and PHSC. The observed crack propagation can be partly attributed to the full dehydration of the matrix. Cavities and fissures are observed throughout the PHSC matrix. At this stage, full C-S-H decomposition was feasible for KFHSC and PHSC.

4 Conclusions

After the analysis the following conclusions can be highlighted:

- Because of the matrix's higher permeability and lower density than those of PHSC, KFHSC experienced a significant decrease in weight and UPV upon exposure to elevated temperatures and a longer exposure period.
- KFHSC in a 1 h exposure reached its maximum strength at 300 °C and maintained it somewhat until 400 °C. The weakening of the concrete material under thermal stress caused more KFHSC compressive strength loss than the degrading impact caused by the fibres.
- In terms of residual splitting tensile strength, the KFHSC samples behaved relatively well with the PHSC samples before 400 ºC, with a significant ductile failure mode for the cube and cylindrical samples, as opposed to the PHSC samples that failed unexpectedly.
- The morphological images agreed closely with the strength characteristics. During the 1 h fire exposure for KFHSC, up to 400 ºC, the kenaf fibre still successfully reduced the crack propagation and thermal incompatibility of the aggregate and cement paste within the matrix, which was an advantage over PHSC samples. Additionally, for the 2 h exposure, this bridging mechanism was maintained until 400 ºC before the matrix completely deteriorated. For a 3 h exposure, the material deterioration began at 400 ºC and continued until 800 ºC, with a significant 'coarsening effect' on the matrices of both mixes at this temperature, both matrices changed from the crystalline to the amorphous phase.
- Based on these discoveries, for an ideal fibre volume fraction of 9 kg/m^3, the application of KFHSC should not be exposed to a temperature exceeding 400 ºC for 3 h exposures.
- Based on microstructural studies, kenaf fibres are advantageous for HSC subjected to high temperatures. In addition to its ability to prevent cracks, the post-cracking stress distribution mitigates the effects of thermal strain caused by the incompatibility of hardened cement paste and aggregates, particularly during the low-temperature phase.

Acknowledgements

The authors express profound gratitude for the support from the Research Management Centre through the HiCOE grant, R.J130000.7822.4J222, and the Technical Staff at the Structure and Materials Laboratory of the School of Civil Engineering, Universiti Teknologi, Malaysia. The financial support received from the Federal Government of Nigeria via TETFund is appreciated.

References

[1] Zeyad, A. M.; Khan, A. H.; Tayeh, B. A. Durability and strength characteristics of high-strength concrete incorporated with volcanic pumice powder and polypropylene fibres.

Journal of Materials Research and Technology, 2020, 9 (1), pp. 806-818. https://doi.org/10.1016/j.jmrt.2019.11.021

[2] Aziz, M. A.; Paramasivam, P.; Lee, S. L. Prospects for natural fibre reinforced concretes in construction. *International Journal of Cement Composites and Lightweight Concrete,* 1981, 3 (2), pp. 123-132. https://doi.org/10.1016/0262-5075(81)90006-3

[3] Elsaid, A.; Dawood, M.; Seracino, R.; Bobko, C. Mechanical properties of kenaf fibre reinforced concrete. *Construction and Building Materials*, 2011, 25 (4), pp. 1991-2001. https://doi.org/10.1016/j.conbuildmat.2010.11.052

[4] Archila, H. et al. Bamboo reinforced concrete: a critical review. *Materials and Structures*, 2018, 51, 102. https://doi.org/10.1617/s11527-018-1228-6

[5] Peng, G.-F. et al. Explosive spalling and residual mechanical properties of fiber-toughened high-performance concrete subjected to high temperatures. *Cement and Concrete Research*, 2006, 36 (4), pp. 723-727. https://doi.org/10.1016/j.cemconres.2005.12.014

[6] Ozawa, M.; Morimoto, H. Effects of various fibres on high-temperature spalling in high-performance concrete. *Construction and Building Materials*, 2014, 71, pp. 83-92. https://doi.org/10.1016/j.conbuildmat.2014.07.068

[7] Moghadam, M. A.; Izadifard, R. A. Effects of steel and glass fibres on mechanical and durability properties of concrete exposed to high temperatures. *Fire Safety Journal*, 2020, 113, 102978. https://doi.org/10.1016/j.firesaf.2020.102978

[8] Ramesh M. Hemp, jute, banana, kenaf, ramie, sisal fibers. In: *Handbook of Properties of Textile and Technical Fibres (Second Edition)*, Bunsell, A, R. (ed.). Woodhead Publishing; 2018, pp. 301-325. https://doi.org/10.1016/b978-0-08-101272-7.00009-2

[9] Ogunbode, E. B. et al. Long-term behaviour of fibrous concrete composite (FCC): A conspectus. *Journal of Advanced Review on Scientific Research*, 2017, 33 (1), pp. 1-12.

[10] Netinger Grubeša, I.; Marković, B.; Gojević, A; Brdarić, J. Effect of hemp fibres on fire resistance of concrete. *Construction and Building Materials*, 2018, 184, pp. 473-484. https://doi.org/10.1016/j.conbuildmat.2018.07.014

[11] Ozawa, M.; et al. Thermal properties of jute fibre concrete at high temperature. *Journal of Structural Fire Engineering*, 2016, 7 (3), pp. 182-192. https://doi.org/10.1108/jsfe-09-2016-017

[12] Zhang, D.; Tan, K. H.; Dasari, A.; Weng, Y. Effect of natural fibers on thermal spalling resistance of ultra-high performance concrete. *Cement and Concrete Composites*, 2020, 109, 103512. https://doi.org/10.1016/j.cemconcomp.2020.103512

[13] Zhao, H. et al. Temperature-adaptive mechanism of bamboo fibers for regulating elevated temperature performance of UHPC. *Construction and Building Materials*, 2025, 471, 140674. https://doi.org/10.1016/j.conbuildmat.2025.140674

[14] Pour, A. K.; Shirkhani, A.; Farsangi, E. N. Spalling resistance and mechanical performance of UHPC under high temperature using hybrid natural and artificial fibers. *Structural engineering and mechanics: An international journal*, 2024, 91 (2), pp. 177-195. https://doi.org/10.12989/sem.2024.91.2.177

[15] Hashim, N. F. et al. Strength and Durability of Kenaf Fibre Reinforced Concrete for Marine Structures. *UMT Journal of Undergraduate Research*, 2019, 1 (1), pp. 113-118. https://doi.org/10.46754/umtjur.v1i1.57

[16] Ogunbode, E. B.; Yatim, J. M.; Yonus, I. M.; Razavi, M. Creep Performance of Kenaf Bio Fibrous Concrete Composite Under Uniaxial Compression. Accessed: November 11, 2025. Available at: https://www.researchgate.net/profile/Jamaludin-Yatim/publication/308740901_CREEP_PERFORMANCE_OF_KENAF_BIO_FIBROUS_CONCRETE_COMPOSITE_UNDER_UNIAXIAL_COMPRESSION/links/58198d4508ae50812f5df9e0/CREEP-PERFORMANCE-OF-KENAF-BIO-FIBROUS-CONCRETE-COMPOSITE-UNDER-UNIAXIAL-COMPRESSION.pdf

[17] Juradin, S.; Vranješ, L. K.; Jozić, D.; Boko, I. Post-Fire Mechanical Properties of Concrete Reinforced with Spanish Broom Fibers. *Journal of Composites Science*, 2021, 5 (10), 265. https://doi.org/10.3390/jcs5100265

[18] Mahjoub, R.; Mohamad, J. M.; Sam, A. R. M.; Hashemi, S. H. Tensile properties of kenaf fiber due to various conditions of chemical fiber surface modifications. *Construction and Building Materials*, 2014, 55, pp. 103-113. https://doi.org/10.1016/j.conbuildmat.2014.01.036

[19] British Standards Institution. BS EN 14889-2:2006. *Fibres for concrete - Part 2: Polymer fibres - Definitions, specifications and conformity*. UK: BSI; 2006.

[20] American Society for Testing and Materials. ASTM C136-06. *Standard Test Method for Sieve Analysis of Fine and Coarse Aggregates*. USA: ASTM; 2006.

[21] American Society for Testing and Materials. ASTM. C494-04. *Standard Specification for Chemical Admixtures for Concrete*. USA: ASTM; 2008.

[22] Aluko, O. G.; Yatim, J. M.; Ab. Kadir, M. A.; Yahya, K. Residual Cube Strength and Microstructural Properties of Fire-Damaged Biofibrous Concrete with GEP-Based Prediction Model. *Arabian Journal for Science and Engineering*, 2023, 48, pp. 13945-13966. https://doi.org/10.1007/s13369-023-08018-x

[23] Fook, L.; Yatim, J. M. An Experimental Study on the Effect of Alkali Treatment on Properties of Kenaf Fibre for Reinforced Concrete Elements. *IJRET: International Journal of Research in Engineering and Technology*, 2015, 04 (08), pp. 37-40. https://doi.org/10.15623/ijret.2015.0408007

[24] Momoh, E. O.; Osofero, A. I. Behaviour of oil palm broom fibres (OPBF) reinforced concrete. *Construction and Building Materials*, 2019, 221, pp. 745-761. https://doi.org/10.1016/j.conbuildmat.2019.06.118

[25] International Organization for Standardization. ISO 834-12. *Fire resistance tests — Elements of building construction*. Switzerland: ISO; 2012.

[26] American Society for Testing and Materials. ASTM E119-16a. *Standard Test Methods for Fire Tests of Building Construction and Materials*. USA: ASTM; 2016.

[27] Liu, M.; Zhao, Y.; Xiao, Y.; Yu, Z. Performance of cement pastes containing sewage sludge ash at elevated temperatures. *Construction and Building Materials*, 2019, 211, pp. 785-795. https://doi.org/10.1016/j.conbuildmat.2019.03.290

[28] Mihoub, I.; Khelifa, M.; Mezhoud, M. Impact of Elevated Temperature on The Properties of Concretes Reinforced. *Civil and Environmental Engineering Reports*, 2020, 30 (3), pp. 161-185. https://doi.org/10.2478/ceer-2020-0038

[29] British Standards Institution. BS 12390-3:2019. *Testing hardened concrete - Compressive strength of test specimens*. UK: BSI; 2019.

[30] British Standards Institution. BS EN 12390-6, *Testing hardened concrete: Tensile splitting strength of test specimens*. UK: BSI; 2009.

[31] Kodur, V. Properties of Concrete at Elevated Temperatures. *International Scholarly Research Notices*, 2014, 2014 (1), 468510. https://doi.org/10.1155/2014/468510

[32] Neville, A. M.; Brooks, J. J. *Concrete Technology*. 2nd Edition, England: Prentice Hall, 2010.

[33] Abdul Awal, A. S. M.; Shehu, I. A. Performance evaluation of concrete containing high volume palm oil fuel ash exposed to elevated temperature. *Construction and Building Materials*, 2015, 76, pp. 214-220. https://doi.org/10.1016/j.conbuildmat.2014.12.001

[34] Heikal, M.; Al-Duaij, O. K.; Ibrahim, N. S. Microstructure of composite cements containing blast-furnace slag and silica nano-particles subjected to elevated thermally treatment temperature. *Construction and Building Materials*, 2015, 93, pp. 1067-1077. https://doi.org/10.1016/j.conbuildmat.2015.05.042

[35] Demirel, B.; Keleştemur, O. Effect of elevated temperature on the mechanical properties of concrete produced with finely ground pumice and silica fume. Fire Safety Journal, 2010, 45 (6-8), pp. 385-391. https://doi.org/10.1016/j.firesaf.2010.08.002

[36] Hager, I. Behaviour of cement concrete at high temperature. *Bulletin of Polish Academy of Technical Sciences*, 2013, 61 (1), pp. 145-154. https://doi.org/10.2478/bpasts-2013-0013

[37] Afshoon, I.; Sharifi, Y. Utilization of micro copper slag in SCC subjected to high temperature. *Journal of Building Engineering*, 2020, 29, 101128. https://doi.org/10.1016/j.jobe.2019.101128

[38] Wang, W.; Lu, C. Li, Y.; Li, Q. An investigation on thermal conductivity of fly ash concrete after elevated temperature exposure. *Construction and Building Materials*, 2017, 148, pp. 148-154. https://doi.org/10.1016/j.conbuildmat.2017.05.068